Defence Science Journal, Vol. 68, No. 5, September 2018, pp. 473-479, DOI : 10.14429/dsj.68.11233

Evaluation of Local Feature Detectors for the Comparison of Thermal and Visual Low Altitude Aerial Images

K. Divya Lakshmi[#], R. Muthaiah[#], K. Kannan[#], and Anand M. Tapas[*]

[#]*Sastra Deemed to be University, Thanjavur – 613 401, India*
[*]*DRDO-Defence Research and Development Laboratory, Hyderabad - 500 058, India*
[*]*E-mail: amtapas@gmail.com*

ABSTRACT

Local features are key regions of an image suitable for applications such as image matching, and fusion. Detection of targets under varying atmospheric conditions, via aerial images is a typical defence application where multi spectral correlation is essential. Focuses on local features for the comparison of thermal and visual aerial images in this study. The state of the art differential and intensity comparison based features are evaluated over the dataset. An improved affine invariant feature is proposed with a new saliency measure. The performances of the existing and the proposed features are measured with a ground truth transformation estimated for each of the image pairs. Among the state of the art local features, speeded up robust feature exhibited the highest average repeatability of 57 per cent. The proposed detector produces features with average repeatability of 64 per cent. Future works include design of techniques for retrieval of corresponding regions.

Keywords: Local features; Aerial images; Thermal images; Image matching; Affine invariant; Image registration

1. INTRODUCTION

Local features are the salient regions of an image characterised by their location and neighbouring region[1]. They are used for applications such as content based image retrieval, motion tracking, image mosaicing, image registration etc, where images captured at different time instances have to be compared robust to the variations caused by the imaging conditions, scene and sensor[2-8]. The major steps for the extraction of local features in the image are - detecting key point locations, formation of neighbourhood region surrounding each of the locations.

Key point locations characterised by spatial co-ordinates, identified in an image have to be repeatable for translation, rotation, view point variations. Various differential methods can be found in the initial works on the key point detection[9-18]. They compute derivatives using neighbourhood region of a pixel to measure its saliency. Scale invariant feature transform (SIFT)[19,20] and speeded up robust features (SURF)[21] are popularly used differential methods that use difference of Gaussian and Determinant of Hessian respectively for key point detection. Smallest univalue segment assimilating nucleus (SUSAN) detector uses a morphological approach for key point detection[22]. The approach is found to be less sensitive to noise and computationally less expensive compared to the differential approaches. Machine learning and heuristic approaches have been used for improving accuracy and computational complexity in features from accelerated segment test (FAST). The algorithm labels a pixel as corner if it is darker or brighter beyond a threshold compared to N contiguous pixels on a circle surrounding it. It uses machine learning to learn optimal values for N and the threshold[23]. Binary robust invariant scalable keypoints (BRISK) applies the FAST detector over a scale space for key point detection[24]. Oriented FAST rotated binary robust independent elementary features (ORB) algorithm assigns an orientation value to the key points detected by FAST[25].

The neighbouring region of a key point detected has to be invariant to uniform or non-uniform scale variations. The selection of the size of the neighbourhood is determined by choosing a scale for the key points detected. The concept of scale space introduced by Lindeberg is used for analysing the images at different scales[26]. The scale space is generated by successive blurring of the image with the Gaussian function. The characteristic scale of the key points can be selected by looking for the local extreme points in the Laplace of Gaussian response across the different scales at the location of the key point[27]. While the Gaussian scale space analysis forms circular neighbourhood invariant to scale variations, approaches to adapt the circular regions to affine invariant elliptical regions are also found in the literature[28-30]. The neighbourhood regions can also be made rotation invariant by computing an orientation for the location based on the pixels in the neighbouring region[20,21,25].

A comparison of affine region detectors is done by Mikolajczyk[31], *et. al*. over a dataset with predominantly planar scenes taken by a single sensor captured from short distances. The work is extended for non planar scenes by Fraundorfer and Bischopf[32]. Johansson[33], *et. al*. evaluate the performance of feature detectors and descriptors for infrared images. Istenic[34],

Received : 15 March 2017, Revised : 09 May 2018
Accepted : 19 July 2018, Online published : 12 September 2018

et. al. perform pre-processing by transforming the intensity values to CIELab colour space and generates edge images using Canny Edge operator for comparison of thermal and visual images with rotation and translation variations. A similar pre-processing is done by Enrique et al where line segments are detected from the edge images using Ramer's algorithm. The feature chosen for registration is triangles formed from the line segments of the images. Affine transformation, which includes translation, rotation, non- uniform scaling is estimated by matching the triangles from both the images[35]. In contrast to edges, texture feature is proposed by Andreja[36] , *et. al*., for the affine registration of thermal and near infrared band images. While the geometric variations as discussed in previous power are minimal, Yahyanejad[7], *et. al*. have attempted registration of thermal and visual images with wide range geometric distortions. Robust Feature Across Edges (RFAE) is proposed in their work for the registration purpose. RFAE converts the images to a binary edge image using Sobel Operator and a variable threshold.

This paper focuses on the performance of various affine and scale invariant feature detectors over a data set of thermal and visual aerial image pairs suffering huge geometric variations. Affine features which are found to handle view point variations effectively[31], were considered for the comparison of the image pairs. The drawback of affine invariant features is that it performs lower than the scale invariant when the scale variations are more dominant than the viewpoint variations[31,41]. A new affine invariant feature detector which exhibits higher repeatability over the predominantly scale variant dataset compared to the state of the art local features, is also discussed in this paper.

2. METHODS AND MATERIALS

The state of the art local features are evaluated using the open source coding available[31,37] and OpenCV, a standard open source package for computer vision.

2.1 Dataset

The dataset comprises pairs of thermal and visual aerial images captured using low altitude unmanned aerial vehicles[7]. The ground truth transformation between each image pair is estimated as homograph matrix from manually selected corresponding points using the Gold standard algorithm.[41] The estimated homograph is validated with the manual corresponding locations and by visually examining the images registered using the homograph. Figure 1 shows a sample of thermal and visual images taken from two different scenes and the thermal image registered to the coordinates of the visual image using the estimated homograph. It can be observed that Scene 1 images contain more textured regions with less number of edges with low curvature and Scene 2 images has more number of high curvature edges.

2.2 Performance measures

Repeatability quantifies the quality of local features extracted from the images. It is the ratio between the number of corresponding features between the images and the smaller of the number of features in the image pair. Corresponding features are identified in two ways – by thresholding overlap error or location error. Overlap error is calculated using Eqn (1).

$$Overlap\_error = 1 - \frac{R_{\mu_A} \cap R_{H^T \mu_B H}}{R_{\mu_A} \cup R_{H^T \mu_B H}} \quad (1)$$

here *A* and *B* are two circular or elliptical features extracted from the visual and thermal images respectively. *H* is the homograph characterising the geometric transformation from thermal to visual image. R_{μ_A} is the region associated with *A*. $R_{H^T \mu_B H}$ is the region of *B* transformed by *H*. Its threshold is fixed at 50 per cent as matching algorithms are designed to tolerate this error. Location error is the distance between the location of *A* and location of *B* transformed using *H*. Its threshold[31] is fixed at 1.5.

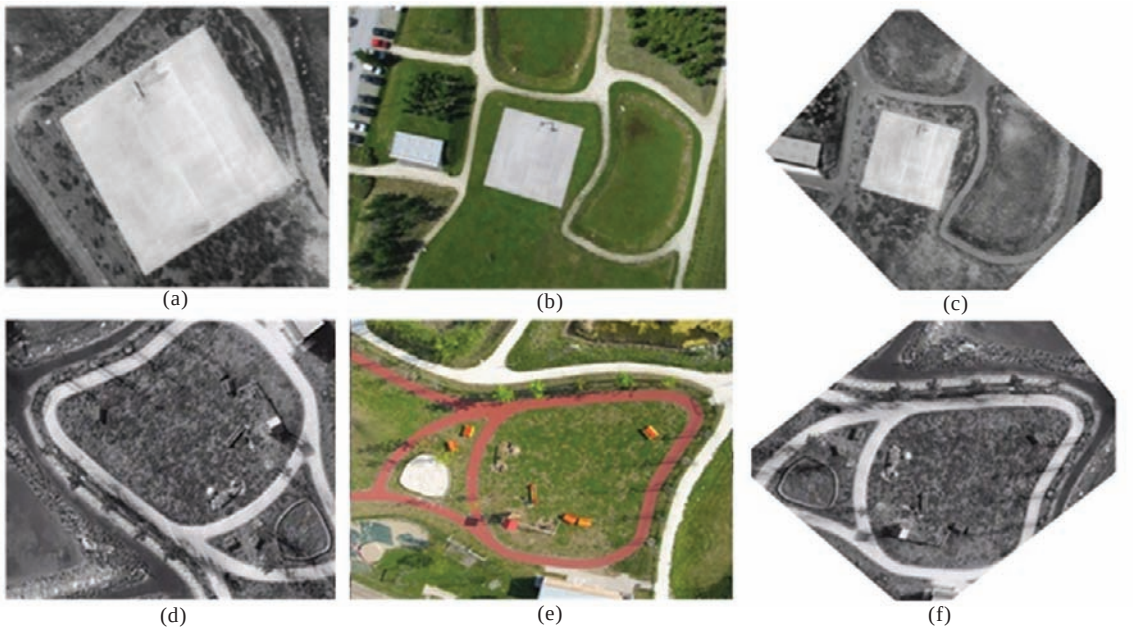

Figure 1. (a) Scene 1 thermal, (b) Scene 1 visual, (c) Scene 1 thermal registered to visual, (d) Scene 2 thermal, (e) Scene 2 visual, (f) Scene 2 thermal registered to visual.

2.3 Hessian Affine Features from Lowe Gaussian Pyramid (HESIFT)

A hybrid multi scale representation is obtained by successively blurring of the base image with Gaussian function and down sampling of the blurred images[21]. The process of blurring and down sampling is repeated till a minimum image size is reached which is the top of the pyramid. For each of the image pixels in the hybrid multi scale representation scale normalised Hessian response is computed as given in Eqn (2).

$$H(x,y,\sigma) = \sigma^2 (L_{xx} L_{yy} - L_{xy}{}^2) \quad (2)$$

$$L_{xx}(x,y) = L(x-1,y) - 2L(x,y) + L(x+1,y) \quad (3)$$

$$L_{yy}(x,y) = L(x,y-1) - 2L(x,y) + L(x,y+1) \quad (4)$$

$$L_{xy}(x,y) = 0.25*(L(x+1,y+1) - L(x+1,y-1) - L(x-1,y+1) + L(x-1,y-1)) \quad (5)$$

here L_{xx}, L_{yy}, L_{xy} are the second order derivatives of the images L in the hybrid multi scale representation, which are obtained by numerical differencing given by Eqns (3-5) [39]. Local extreme points are identified from the Hessian scale space. Edge points are eliminated by removing points with ratio between principle curvatures less than 10[21]. The spatial coordinates (x, y) and the scale values (σ) of the key points filtered are fine tuned to higher accuracy by solving the first order derivative of the Taylor series expansion of the Hessian function obtained from its neighbourhood. Elliptical region is formed from the circular neighbouring region whose radius is proportional to the scale of the key point. It is formed by transforming the circular region using its second moment matrix till the ratio of the Eigen values reaches unity[12].

2.4 Proposed saliency measure

A new saliency measure which replaces the Hessian measure of Eqn (5) in the above methodology is as given in Eqn (6).

$$C(x,y,\sigma) = \sigma^2 (L_x L_y - L_d{}^2) \quad (6)$$

here C is the proposed saliency measure for a pixel whose location is x, y in the pyramid image of scale σ. It is based on the first derivative filtering of the image in the x, y directions and also in the diagonal direction d. The filters used for obtaining the derivative images are as given in Eqns (7-9).

$$F_x = \begin{bmatrix} -1 & 0 & 1 \\ -1 & 0 & 1 \\ -1 & 0 & 1 \end{bmatrix} \quad (7)$$

$$F_y = \begin{bmatrix} -1 & -1 & -1 \\ 0 & 0 & 0 \\ 1 & 1 & 1 \end{bmatrix} \quad (8)$$

$$F_d = \begin{bmatrix} -1 & 0 & -1 \\ 0 & 0 & 0 \\ 1 & 0 & 1 \end{bmatrix} \quad (9)$$

here F_x, F_y, and F_d are the filters that have to be convolved with the image to obtain L_x, L_y, and L_d respectively. While F_x and F_y are Prewitt's operators[40] to obtain horizontal and vertical edges in the image respectively, the filter F_d introduced in this paper calculates the numerical differences of the neighbouring pixels in the diagonal directions. The derivatives of the proposed measure also involve more number (4 to 6) of neighbours for the computation of the saliency of a pixel than the Hessian derivatives which involves two to four neighbours in addition to the pixel value.

3. RESULTS AND DISCUSSIONS

3.1 Impact of the Proposed Saliency Measure

Figure 2 shows the results of the Hessian response and the proposed saliency measure for the pixels of the first level of the scale space pyramid. It can be observed that the proposed measure has enhanced the fine details and edges of the images. Thus more repeatable features are returned by the proposed saliency measure when implemented in the framework of HESIFT replacing the Hessian response. The impact of replacing the response was also evaluated over twenty pairs of thermal and visual images[7] which includes non planar scenes in addition to the scene images considered and the proposed measure has improved the performance by 18 per cent on an average.

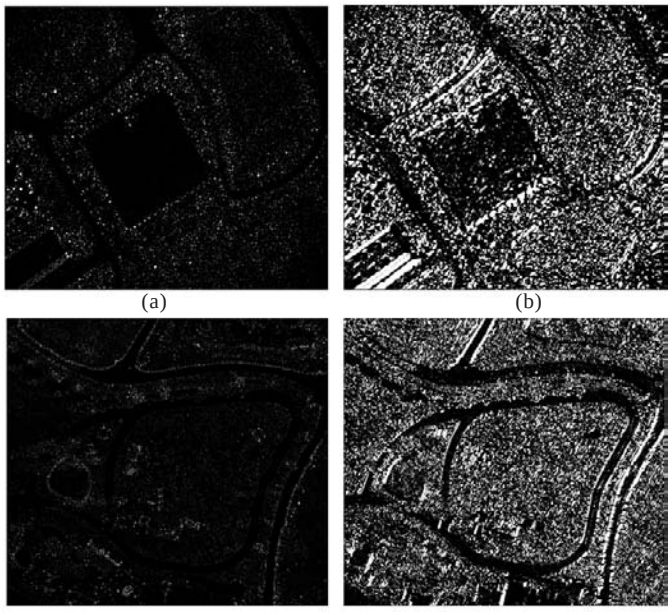

Figure 2. Edge maps Scene 1 Image (a) Hessian response (b) Proposed measure scene 2 image (c) Hessian response (d) Proposed measure.

3.2 Repeatability Obtained from Overlap Error based Correspondences

Table 1 shows the average values of the performance measures obtained over the dataset of six pairs of thermal and visual images. Standard parameters are set to obtain features from various detectors. It has been experimentally demonstrated that beyond a level count of features does not impact the repeatability which is more algorithm dependent [31] and thus is not studied in this research.

It can be observed that features extracted with the proposed saliency measure have obtained the highest number of correspondences and repeatability value which is 7 per cent higher than the existing state of the art feature SURF for a similar count of features extracted from the images. It is found in the literature[38] that the affine features perform poorly when affine variations are dominated by scale and rotation variations. This can be observed in the results where the performance of Harris affine and Hessian affine is lower compared to the scale invariant features – Harris Laplace, Hessian Laplace, SURF, ORB, BRISK. It can also be observed from the images in the dataset shown in Fig. 1 that scale and rotation variations are more prominent compared to the view point variations. The HESIFT feature, though it extracts affine regions, exhibits higher repeatability than the standard affine features Harris and Hessian affine. This performance can be contributed to the multi scale hybrid pyramid construction compared to the scale space representation in the Harris and Hessian affine detectors.

Table 1. Average performance measures obtained over the dataset

Feature	Count thermal feature	Count visual feature	Corresponding feature	Repeatability
SURF	2541.00	4613.83	1469.50	57.01
SIFT	4333.67	3631.33	199.17	6.53
ORB	4916.50	4375.33	1528.00	35.11
FAST	2844.83	4956.17	375.50	16.82
BRISK	1838.83	3916.83	792.83	44.17
HALAP	404.67	576.83	97.67	23.43
HELAP	2393.83	4156.50	1061.00	43.63
HAAFF	394.83	569.83	80.33	19.90
HEAFF	1681.17	2735.67	448.50	26.16
HESIFT	2047.67	3164.17	820.33	42.16
Proposed	2991.50	6169.17	1851.83	64.20

Tables 2 shows the repeatability value of the features detected for various values of the overlap surface error between the features extracted from the four pairs of images of scene 1.

It can be observed that the proposed feature exhibits highest repeatability among the features studied for overlap error of 50 per cent. The repeatability was the highest for the ORB features when the overlap error is less than 40 per cent. In a few cases SURF and BRISK were found to exhibit highest repeatability which is closer to the repeatability of ORB or the proposed feature. Though improvement in repeatability is marginal, it will result in higher precision in matching and in turn would improve the success rate of applications such as object detection.

Table 3 shows the repeatability values of features extracted from image pairs of scene 2.

Again, it can be observed from Table 3 that ORB gives the best repeatability results for lower overlap errors and the proposed feature gives the best repeatability results for higher overlap errors for image pairs of scene 2. For all the values of overlap error, the repeatability of the proposed feature is higher than the HESIFT implementation. From this we can infer the positive impact of diagonal differencing introduced in the saliency measure used for detecting salient regions.

Table 2. Average repeatability for image pairs of scene 1

Feature	Repeatability (%) for overlap errors (%)					
	<10	<20	<30	<40	<50	<60
BRISK	0.51	4.32	21.01	39.01	50.31	58.55
SURF	1.51	9.76	25.92	42.88	53.22	59.42
SIFT	0	0.23	1.28	3.02	6.92	13.33
ORB	14.06	28.54	35.46	38.82	41.49	43.70
FAST	0	0.70	14.72	21.60	26.85	31.35
HESIFT	0	3.26	14.74	31.60	44.79	53.26
HESLAP	1.01	9.01	20.39	31.17	41.49	50.60
HESAFF	0.08	2.02	7.39	17.10	27.71	39.21
HARLAP	0.49	4.17	12.26	20.59	29.66	36.52
HARAFF	0	0.25	5.74	15.71	25.69	35.66
Proposed	0.26	5.54	21.65	42.68	55.36	63.25

Table 3. Average repeatability for image pairs of scene 2

Feature	Average repeatability (%) for overlap errors (%)					
	<10	<20	<30	<40	<50	<60
BRISK	0.81	6.63	19.66	34.62	47.52	56.68
SURF	1.37	9.30	23.08	37.47	46.98	53.17
SIFT	0.02	0.47	1.61	3.32	6.61	11.59
ORB	7.75	20.02	26.14	29.80	33.33	36.86
FAST	0.21	1.88	7.18	14.04	21.63	26.31
HESIFT	0.14	2.22	9.20	19.41	28.43	35.17
HESLAP	1.85	10.77	21.10	30.87	40.17	47.43
HESAFF	0.27	2.69	6.47	12.44	19.68	27.40
HARLAP	2.06	8.43	14.00	18.67	23.64	27.78
HARAFF	0.16	3.61	9.55	15.44	20.35	25.85
Proposed	0.23	4.80	21.30	42.04	55.39	62.87

3.3 Repeatability Obtained from Location Error based Correspondences

Table 4 shows the average repeatability values obtained for features extracted from the six pair of images of the dataset. It can be observed that the ORB feature produces the highest number of correspondences where location error is less than 1.5 pixels. This can be attributed to the higher repeatability of the ORB features for overlap error less than 30 per cent, which is observed in the Tables 2 and 3. The number of correspondences produced by the proposed feature is the second highest among the features detected over the dataset. The proposed measure also returns more corresponding features and repeatability (3% higher) compared to the FAST method which requires an additional learning step and relies on intensity comparisons. [23]

Table 4. Average repeatability based on location error

Feature	Average count thermal feature	Average count visual feature	Average corresponding features
SURF	2541.00	4613.83	160.00
SIFT	4333.67	3631.33	203.67
BRISK	1838.83	3916.83	100.83
FAST	2844.83	4956.17	148.67
ORB	4916.50	4375.33	599.00
HALAP	404.67	576.83	30.50
HELAP	2393.83	4156.50	236.50
HAAFF	394.83	569.83	30.50
HEAFF	1748.33	3226.83	102.33
HESIFT	2047.67	3164.17	95.67
Proposed	2991.50	6169.17	244.17

4. CONCLUSIONS

This paper concludes that the proposed saliency measure which involves differencing in the diagonal direction has improved the performance of the Pedroch implementation by around 18 per cent over a set of twenty thermal visual image pairs[7]. It is also found to possess higher repeatability for overlap error greater than 40 per cent when compared to the recent detectors such as ORB, FAST and BRISK. However, when the location error is taken into consideration ORB feature performs the best compared to the other features. The proposed feature can be used for applications that use robust descriptors for matching whereas ORB can be used for the applications such as 3D reconstruction that require high precision in the location of the corresponding points. The local features detected in the images have to be described by suitable vectors. The vectors should be robust to geometric and photometric variations and distinctive for it to be successfully matched with the corresponding feature. Development of a description and matching algorithm for the successful retrieval of the repeatable features are the future directions of research for the work is presented in this study.

REFERENCES

1. Tuytelaars, T. & Mikolajczyk, K. Local invariant feature detectors: A survey. *Comput. Graphics Vision*, 2008, **3**(3), 177–280.
2. Gao, K.; Lin, S.; Zhang, Y.; Tang, S. & Ren, H. Attention model based SIFT keypoints filtration for image retrieval, *In* Proceedings of the 7th IEEE/ACIS International Conference on Computer and Information Science IEEE/ ACIS ICIS 2008, 14-16 May 2008, Portland, OR, USA, pp. 191–196.
3. Liu, X.; Shao, Z. & Liu, J. Ontology-based image retrieval with SIFT features, *In* Proceedings of the 1st International Conference on Pervasive Computing, Signal Processing and Applications, PCSPA 2010, 17-19 Sep 2010, Harbin, China, pp. 464–467, doi: 10.1109/PCSPA.2010.118
4. Velmurugan, K. & Baboo, S. S. Content-Based Image Retrieval using SURF and Colour Moments. *Global J. Comput. Sci. Technol.*, 2011, **11**(10), 1–4.
5. Kim, Y. D.; Park, J. T.; Moon, I. Y. & Oh, C. H. Performance analysis of ORB image matching based on android. *Int. J. Software Eng. Applications*, 2014, **8**(3), 11–20.
6. Li, H.; Dong, Y.; He, X.; Xie, S. & Luo, J. A sonar image mosaicing algorithm based on improved SIFT for USV, *In* 2014 IEEE International Conference on Mechatronics and Automation, IEEE ICMA 2014, 3-6 Aug 2014,Tianjin, China, pp. 1839–1843. doi: 10.1109/ICMA.2014.6885981
7. Yahyanejad, S. & Rinner, B. A fast and mobile system for registration of low-altitude visual and thermal aerial images using multiple small-scale UAVs. *ISPRS J. Photogrammetry Remote Sensing*,2015, **104**, 189–202.
8. Brown, L. G. A survey of image registration techniques. *ACM Computing Surveys*, 1992, **24**(4), 325–376.
9. Morevac, H. Obstacle Avoidance and Navigation in the Real World by a Seeing Robot Rover, Carnegie-Mellon University, Robotics Institute, Report No. CMU-RI-TR-3, September 1980.
10. Harris, C. & Stephens, M. A Combined Corner and Edge Detector, *In* Procedings of the Alvey Vision Conference 1988, 31 Aug-2 Sep 1988, Manchester, UK, pp. 147–151. doi: 10.5244/C.2.23
11. Li, Z. & Shen, Y. A robust corner detector based on curvature scale space and Harris. *In* Proceedings of 2011 International Conference on Image Analysis and Signal Processing, IASP 2011, 21-23 Oct 2011, Hubei, China, pp. 223–226. doi: 10.1109/IASP.2011.6109034
12. Ryu, J.-B.; Park, H.-H. & Park, J. Corner classification using Harris algorithm. *Electronics Letters*, 2011, **47**(9), 536.
13. Bellavia, F.; Tegolo, D. & Valenti, C. Improving Harris corner selection strategy. *IET Computer Vision*, 2011, **5**(2), 87.
14. Gueguen, L. & Pesaresi, M. Multi scale Harris corner detector based on differential morphological decomposition. *Pattern Recognition Letters*, 2011, **32**(14), 1714–1719.
15. P. Beaudet, Rotationally invariant image operators. *In* Proceedings of the 4th International Joint Conference on Pattern Recognition, 7-10 Nov, 1978, Kyoto, Japan, pp. 579–583.
16. Kitchen, L. & Rosenfeld, A. Gray-level corner detection. *Pattern Recognition Letters*,1982, **1**(2), 95–102.
17. Wang, H. & Brady, M. Real-time corner detection algorithm for motion estimation. *Image Vision Comput.*,1995, **13**(9), 695–703.
18. Zuniga O. A. and Haralick, R.M. Corner detection using the facet model. *In* Proceedings of Conference on Computer Vision and Pattern Recognition, Jun 1983, Washington D.C.,US, pp. 30–37.
19. Lowe, D. G. Object recognition from local scale-invariant features, *In* Proceedings of the Seventh IEEE

International Conference on Computer Vision, 20-27 Sep 1999, Kerkyra, Greece, **2**(8), pp. 1150–1157. doi: 10.1109/ICCV.1999.790410

20. Lowe, D. G. Distinctive image features from scale-invariant keypoints. *Int. J. Comput. Vision*, 2004, **60**(2), 91–110. doi: 10.1023/B:VISI.0000029664.99615.94
21. Bay, H.; Tuytelaars, T. & Van Gool, L. Speeded up robust features (SURF). *Comput. Vision Image Understanding*, 2008, **110**(3), 346-359.
22. Smith, S. & Brady, J. SUSAN—a new approach to low level image processing. *Int. J. Comput. Vision*,1997, **23**(1), 45–78.
23. Rosten, E.; Porter, R. & Drummond, T. Faster and better: A machine learning approach to corner detection. *IEEE Trans. Pattern Anal. Mach. Intelligence*, 2010, **32**(1), 105–119.
24. Leutenegger, S.; Chli, M. & Siegwart, R. Y. BRISK: Binary robust invariant scalable keypoints. In Proceedings of the 2011 IEEE International Conference on Computer Vision, 6-13 Nov 2011, Barcelone, Spain, pp. 2548–2555. doi: 10.1109/ICCV.2011.6126542
25. Rublee, E.; Rabaud, V.; Konolige, K. & Bradski, G. ORB: An efficient alternative to SIFT or SURF, *In* Proceedings of the 2011 IEEE International Conference on Computer Vision, 6-13 Nov 2011, Barcelona, Spain, pp. 2564–2571. doi: 10.1109/ICCV.2011.6126544
26. Lindeberg, T. Scale-space for discrete signals. *IEEE Trans. Pattern Anal. Mach. Intelligence*, 1990, **12**(3), 234–254.
27. Lindeberg, T. Feature detection with automatic scale selection. *Int. J. Comput. Vision*, 1998, **30**(2), 79–116. doi: 10.1023/A:1008045108935
28. Lindeberg, T. & Gårding, J. Shape-adapted smoothing in estimation of 3-D shape cues from affine deformations of local 2-D brightness structure. *Image Vision Comput.*, 1997, **15**(6), 415–434.
29. Baumberg, A. Reliable feature matching across widely separated views. In Proceedings of the 2000 IEEE International Conference on Computer Vision and Pattern Recognition, 13-15 June 2000, SC, USA, pp. 774-781. doi: 10.1109/CVPR.2000.855899
30. Mikolajczyk, K. & Schmid, C. Scale & affine invariant interest point detectors. *Int. J. Comput. Vision*, 2004, **60**(1), 63–86.
31. Mikolajczyk, K.; Tuytelaars, T.; Schmid, C.; Zisserman, A.; Matas, J.; Schaffalitzky, F. & Van Gool, L. A comparison of affine region detectors. *Int. J. Comput. Vision*, 2005, **65**(1–2), 43–72.
32. Fraundorfer, F. & Bischof, H. A novel performance evaluation method of local detectors on non-planar scenes. *In* 2005 IEEE Computer Society Conference on Computer Vision and Pattern Recognition (CVPR'05) - Workshops, 21-23 Sep 2005, CA, USA, pp.33-33. doi: 10.1109/CVPR.2005.393
33. Johansson, J.; Solli, M. & Maki, A. An evaluation of local feature detectors and descriptors for infrared images. *In* Computer Vision - European Conference on Computer Vision 2016 Workshop, 8-10 and 14-16 Oct 2016, Amsterdam, Netherlands, pp.711-23.
34. Istenic, R.; Heric, D.; Ribaric, S. & Zazula, D. Thermal and visual image registration in hough parameter space. *In* 14th International Workshop on Systems, Signals and Image Processing and 6th EURASIP Conference Focused on Speech and Image Processing, Multimedia Communications and Services, 27-30 Jun 2007, Maribor, Slovenia, pp. 106–109. doi: 10.1109/IWSSIP.2007.4381164
35. Coiras, E.; Santamaría, J. & Miravet, C. Segment-based registration technique for visual-infrared images. *Optical Engineering*, **39**(1), 282. doi: 10.1117/1.602363
36. Jarc, A.; Pers, J.; Rogelj, P.; Perse, M. & Kovacic, S. Texture features for affine registration of thermal(FLIR) and visible images. *In* Proceedings of the 12th Computer Vision Winter Workshop, 6-8 Feb 2007, St.Lambrecht, Austria, pp. 35-42.
37. Perd'och, M.; Chum, O. & Matas, J. Efficient representation of local geometry for large scale object retrieval. *In* 2009 IEEE Computer Society Conference on Computer Vision and Pattern Recognition Workshops, CVPR Workshops 2009, 20-26 Jun 2009, FL, USA, pp. 9–16. doi: 10.1109/CVPRW.2009.5206529
38. Hartley, R. & Zisserman, A. Multiple View Geometry in Computer Vision, Cambridge University Press, New York, US, 2004, 673p.
39. Gonzalez, R.C. & Woods, R.E. Digital Image Processing, Prentice Hall, New Jersey, US, 2002, 793p.
40. Prewitt, J. Object enhancement and extraction, *Picture Processing and Psychopictorics*, 1970, **10**(1), 15-19.
41. Bhatia, A. Hessian-Laplace feature detector and Haar descriptor for image matching, University of Ottawa, Ottawa, Canada, 2007. (PhD Thesis).

ACKNOWLEDGEMENTS

This work was supported by the Council of Scientific and Industrial Research, the premier research and development organisation in India, under the Senior Research Fellowship Scheme. (Grant number 09/1095/(0009) /2015-EMR-I). The third author wishes to thank Department of Science & Technology - Science and Engineering Research Board for the financial support through FIST No.: SR/FST/MSI-107/2015 and TATA Reality IT city-SASTRA Srinivasan Ramanujan Research Cell.

CONTRIBUTORS

Ms Divya Lakshmi K. is currently doing her full time research in Image Registration at School of Computing SASTRA Deemed to be University, Thanjavur. She received B.E (Electronics and Communication) and ME (Computer Science Engineering with specialisation in Knowledge Engineering and Computational Linguistics). Her interests include programming, image processing and machine learning.

In the current study, she contributed to the design of the feature detectors, their software implementation and testing.

Mr R. Muthaiah is working as Professor in SASTRA Deemed to be University, Thanjavur, India. He has around 50 International Journal papers and 5 International Conference papers. He is a member of IE and AECE. His research interest includes image processing, VLSI and Network Security.
In the current study, he contributed to the literature survey, data collection.

Mr Kannan K. is working as Professor (Department of Mathematics), Dean, School of Humanities and Sciences, in SASTRA University, Thanjavur, India. He is a member of the Ramanujam Mathematical Society. His research interest includes image processing, hypergraphs.
He contributed to the analysis of the results and the mathematical basics behind the feature detectors.

Mr Anand M. Tapas is working as a Scientist at the Defence Research Development Laboratory, Hyderabad. Earlier, he had worked in Research Centre Imarat, Hyderabad and Automation Division of TISCO and Radio Astronomy Group of TIFR. He is involved in system engineering and simulations.
He provided the initial idea for the study and helped to shape the research, analysis and manuscript.